Science Signaling
AAAS

` Bruton's Tyrosine Kinase Revealed as a Negative Regulator of Wnt-{beta}-Catenin Signaling

Richard G. James, Travis L. Biechele, William H. Conrad, Nathan D. Camp, Daniel M. Fass, Michael B. Major, Karen Sommer, XianHua Yi, Brian S. Roberts, Michele A. Cleary, William T. Arthur, Michael MacCoss, David J. Rawlings, Stephen J. Haggarty and Randall T. Moon (26 May 2009)
Science Signaling **2** (72), ra25. [DOI: 10.1126/scisignal.2000230]

Science Signaling (ISSN 1937-9145) is published weekly, except the last week in December, by the American Association for the Advancement of Science, 1200 New York Avenue, NW, Washington, DC 20005.

CELL BIOLOGY

Bruton's Tyrosine Kinase Revealed as a Negative Regulator of Wnt–β-Catenin Signaling

Richard G. James,[1,2*] Travis L. Biechele,[1,2*] William H. Conrad,[1,2] Nathan D. Camp,[1,2] Daniel M. Fass,[3†] Michael B. Major,[1,2] Karen Sommer,[4] XianHua Yi,[5] Brian S. Roberts,[6] Michele A. Cleary,[6] William T. Arthur,[6] Michael MacCoss,[5] David J. Rawlings,[4] Stephen J. Haggarty,[3†] Randall T. Moon[1,2‡]

(Published 26 May 2009; Volume 2 Issue 72 ra25)

Wnts are secreted ligands that activate several receptor-mediated signal transduction cascades. Homeostatic Wnt signaling through β-catenin is required in adults, because either elevation or attenuation of β-catenin function has been linked to diverse diseases. To contribute to the identification of both protein and pharmacological regulators of this pathway, we describe a combinatorial screen that merged data from a high-throughput screen of known bioactive compounds with an independent focused small interfering RNA screen. Each screen independently revealed Bruton's tyrosine kinase (BTK) as an inhibitor of Wnt–β-catenin signaling. Loss of *BTK* function in human colorectal cancer cells, human B cells, zebrafish embryos, and cells derived from X-linked agammaglobulinemia patients with a mutant *BTK* gene resulted in elevated Wnt–β-catenin signaling, confirming that BTK acts as a negative regulator of this pathway. From affinity purification–mass spectrometry and biochemical binding studies, we found that BTK directly interacts with a nuclear component of Wnt–β-catenin signaling, CDC73. Further, we show that BTK increased the abundance of CDC73 in the absence of stimulation and that CDC73 acted as a repressor of β-catenin–mediated transcription in human colorectal cancer cells and B cells.

INTRODUCTION

Wnts are a multigene family of secreted ligands that bind to serpentine Frizzled receptors and in some contexts to LRP5 or LRP6 co-receptors to activate multiple downstream signaling pathways. The Wnt pathway that signals through β-catenin (Wnt–β-catenin pathway) is integral to vertebrate development, to tissue homeostasis in adults, and to disease processes (*1*). For example, constitutive Wnt–β-catenin signaling is linked to many cancers, including acute lymphoblastic leukemia (*2*, *3*) and colorectal cancer (*3*, *4*), whereas attenuated Wnt–β-catenin signaling is linked to bone density syndromes (*5*) and to neurodegeneration (*6*).

The activity of the Wnt–β-catenin pathway is dependent on the abundance of β-catenin (encoded by the *CTNNB1* in mammals), which is regulated by a "destruction complex" containing the scaffolding proteins AXIN and APC. This destruction complex enhances the phosphorylation of CTNNB1 by GSK3β (glycogen synthase kinase 3β), thus targeting it for ubiquitin-mediated degradation by the proteasome. Wnt stimulation leads to inhibition of GSK3β and, therefore, to stabilization of CTNNB1. Following accumulation in the cytosol, CTNNB1 is transported to the nucleus, where it associates with numerous proteins, including the HMG box transcription factors TCF and LEF (T cell factor and lymphoid enhancer factor, respectively) [reviewed in (*7*, *8*)], and the PAF (polymerase-associated factor) transcriptional elongation complex members CDC73 and LEO1 (*9*). CTNNB1 then stimulates transcription of target genes associated with cell growth, survival, differentiation, and stem cell self-renewal.

Small interfering RNA (siRNA) screens, small-molecule screens, and proteomic screens (*10*–*15*) continue to identify regulators of Wnt–β-catenin signaling, perhaps hinting at the existence of cell type–specific or context-dependent modulators of the pathway. Part of the difficulty in establishing broadly acceptable criteria for identifying the components of a signaling network even within a specific cellular context is that individual screens are limited by the need to impose somewhat arbitrary cutoff limits for further consideration of prospective hits and by the need to then conduct time-consuming validation assays of those prospective hits. This led us to consider that a combinatorial screen that integrates both chemical genetic and siRNA approaches might reduce the impact of off-target effects specific to each individual screening technique and thereby provide high-confidence independent validation of previously unidentified protein modulators of the Wnt–β-catenin.

Here, we present the integration of a high-throughput, small-molecule screen and a focused siRNA screen of the Wnt–β-catenin pathway. In addition to confirming several previously published hits, each screen independently identified several previously unrecognized regulators of Wnt–β-catenin signaling, including the identification of the B cell kinase, Bruton's tyrosine kinase (BTK), as an inhibitor of Wnt–β-catenin signaling. We then focused on the mechanisms of this activity, revealing that BTK stabilized CDC73, which then acted as a B cell–specific inhibitor of β-catenin–dependent transcription.

RESULTS

Integrating siRNA and small-molecule screening reveals previously unknown Wnt–β-catenin signaling regulators

We integrated the results of an independent siRNA screen and a small-molecule, high-throughput screen (Fig. 1A), with the expectation that

[1]Department of Pharmacology, Howard Hughes Medical Institute, University of Washington School of Medicine, Box 357370, Seattle, WA 98195, USA. [2]Institute for Stem Cell and Regenerative Medicine, University of Washington School of Medicine, Box 357370, Seattle, WA 98195, USA. [3]The Broad Institute of Harvard University and Massachusetts Institute of Technology, 7 Cambridge Street, Cambridge, MA 02141, USA. [4]Departments of Pediatrics and Immunology, Seattle Children's Research Institute, 1900 Ninth Avenue, C9S-7, Seattle, WA 98101, USA. [5]Department of Genome Sciences, University of Washington School of Medicine, Seattle, WA 98195, USA. [6]Rosetta Inpharmatics, LLC, a wholly owned subsidiary of Merck & Co Inc., 401 Terry Avenue N, Seattle, WA 98109, USA.
*These authors contributed equally to this work.
†Present address: Center for Human Genetic Research, Massachusetts General Hospital, 185 Cambridge Street, Boston, MA 02114, USA.
‡To whom correspondence should be addressed. E-mail: rtmoon@u.washington.edu

integrating multiple screens would compensate for some of the deficiencies inherent in any single screen and thereby rapidly identify and validate previously unknown modulators of the Wnt–β-catenin pathway. A small-molecule screen was performed in murine HT22 neuronal cells stably infected with a β-catenin–activated luciferase reporter (BAR) (*16*). Cells treated with a median effective concentration (EC_{50}) dose of WNT3A were screened with 3884 known bioactive compounds to identify molecules that increased or decreased BAR activity relative to dimethyl sulfoxide (DMSO)–treated controls. Independently, human RKO colonocyte cells transduced with the lentiviral BAR reporter (RKO:BAR) were similarly subjected to an EC_{50} dose of WNT3A after transfection with siRNA pools, targeting 2518 genes, most of which encoded proteins with enzymatic activity or were genes linked to disease. One hundred and thirty-nine known bioactive molecules (Databases S1 and S4) and 446 siRNA pools (Databases S2, S3, and S5) met our hit criteria (see Materials and Methods) for significantly increasing luciferase expression in the presence of WNT3A.

We compared the results from the small-molecule screen and the siRNA screen to determine which proteins were independently identified in both screens. To generate a list of possible protein targets of the hits found in the chemical screen, we used the manually curated database of small molecule–protein interactions and algorithms provided by the Search Tool for Interactions of Chemicals (STITCH) (*17*). STITCH identified 292 proteins reported to interact with or be regulated by the small molecules that were hits in our primary screen (Databases S6 and S13). Integration of the 292 protein targets of the small-molecule screen with the 446 targets of the siRNA screen revealed 34 protein targets (Fig. 1B and Table 1) that were

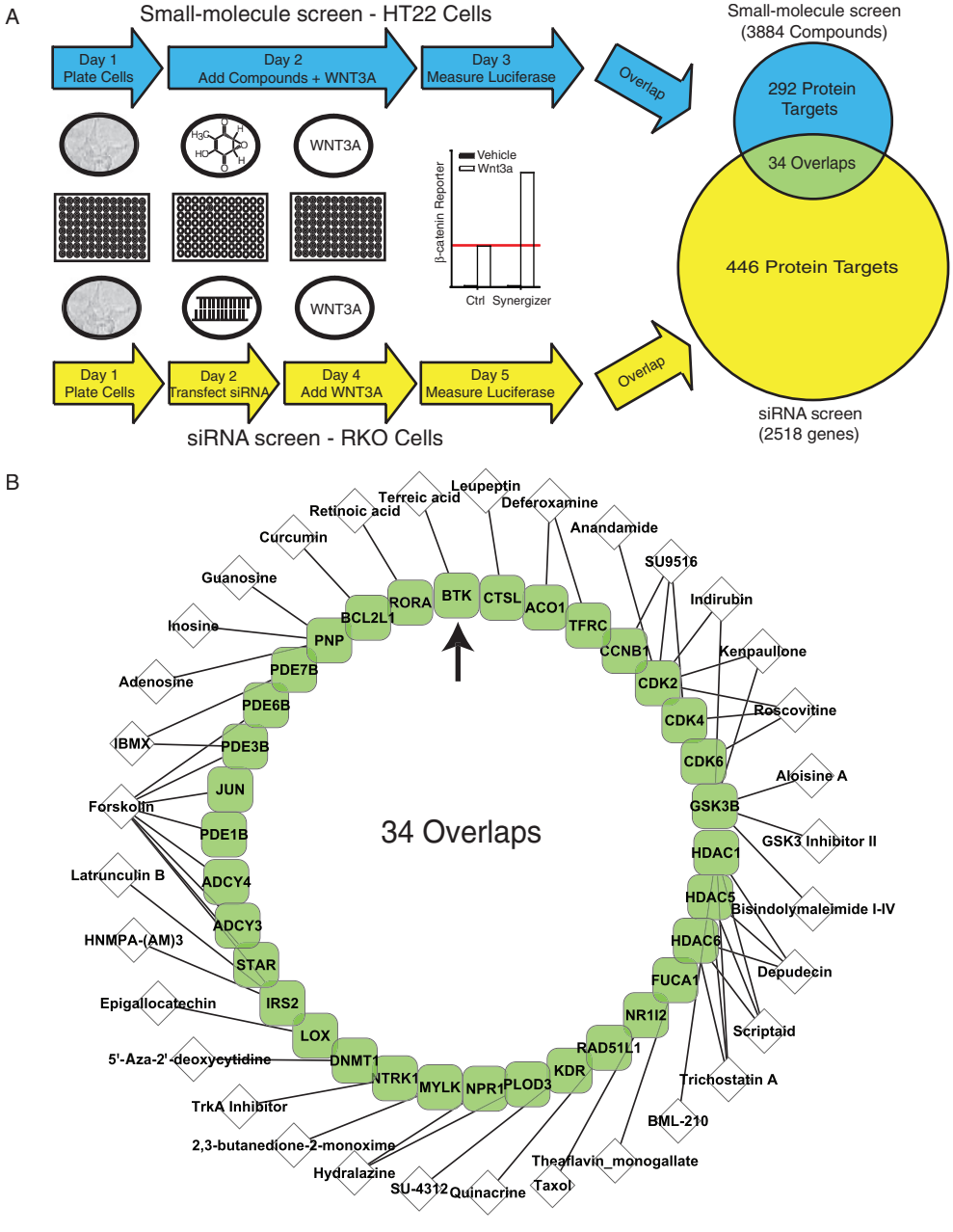

Fig. 1. (A) Schematic of combinatorial small-molecule and siRNA screening strategy. The flow chart shows the time course of the small-molecule and siRNA screens. See Results section for an explanation of the overlap process. (B) The 34 overlaps were proteins independently targeted by hits in both the siRNA and small-molecule screens (green, square nodes represent the 34 overlaps). White diamond nodes represent the small molecules that are associated with the 34 overlaps, and the black edges signify interactions between the small molecules and the proteins. IBMX, 3-isobutyl-1-methylxanthine.

Table 1. Proteins encoded by the genes that were positive in both the siRNA screen and were targets of the small-molecule screen hits. Proteins are listed in alphabetical order by name.

Overlap (protein)	Fold change siRNA	Small molecule	Z-score small molecule
ACO1	3.35	Deferoxamine	4.71
ADCY4	3.54	Forskolin	48.1
BCL2L1	2.10	Curcumin	22.6
BTK	2.74	Terreic acid	15.2
CCNB1	2.43	SU9516	5.86
CDK2	2.20	Anandamide	7.56
		Indirubin	8.90
		Kenpaullone	23.0
		Roscovitine	3.31
		SU9516	5.86
CDK4	2.39	Roscovitine	3.31
		SU9516	5.86
CDK6	2.09	Roscovitine	3.31
CTSL	3.43	Leupeptin	3.45
DNMT1	5.50	5′-Aza-2′-deoxycytidine	26.1
ENSP00000276449	2.73	Forskolin	48.1
ENSP00000354532	2.05	Adenosine	6.08
		Guanosine	2.97
		Inosine	5.25
FUCA1	2.13	Theaflavin monogallate	6.12
GSK3B	2.33	Aloisine A	6.54
		Bisindolymaleimide I-IV	24.8
		GSK-3 inhibitor II	5.76
		Indirubin	8.90
		Kenpaullone	23.0
HDAC1	5.98	BML-210	46.0
		Depudecin	35.0
		Scriptaid	162
		Trichostatin A	74.0
HDAC5	2.71	Depudecin	35.0
		Scriptaid	162
		Trichostatin A	74.0
HDAC6	3.42	Depudecin	35.0
		Scriptaid	162
		Trichostatin A	74.0
IRS2	2.59	Latrunculin B	69.3
		Forskolin	48.1
		HNMPA-(AM)3	13.3
JUN	2.13	Forskolin	48.1
KDR	2.58	SU-4312	3.56
KIAA0511	2.34	Forskolin	48.1
LOX	2.41	Epigallocatechin	22.0
MYLK	2.20	2,3-Butanedione-2-monoxime	7.23
NPR1	2.05	Hydralazine	3.28
NR1I2	3.90	Taxol	7.53
NTRK1	2.25	TrkA inhibitor	6.25
PDE1B	2.12	Forskolin	48.1
PDE3B	2.19	Forskolin	48.1
		IBMX	4.36
PDE6B	3.17	Forskolin	48.1
PDE7B	7.91	IBMX	4.36
PLOD3	2.24	Hydralazine	3.28
RAD51L1	5.26	Quinacrine	21.8
RORA	0.49	Retinoic acid	14.3
TFRC	2.64	Deferoxamine	4.71

independently identified in the small-molecule and the siRNA screen as regulating the Wnt–β-catenin signaling pathway. Among the 34 proteins identified in our integrated screen are several previously reported regulators of the Wnt–β-catenin signal transduction cascade, including GSK3β (*18*), histone deacetylases (*19*), and phosphodiesterases (*20*), thus validating the approach.

Small molecules can target functionally redundant proteins or those that are difficult to reduce effectively with siRNA knockdown. Because many proteins function in protein complexes, it is possible to use bioinformatics combined with screen integration to recover protein targets that would be false negatives in siRNA screens conducted in isolation. To expand our integration to include both protein targets of siRNA hits and their binding partners, we used the Search Tool for the Retrieval of Interacting Genes/Proteins (STRING) (*21*). This identified 1855 proteins (rectangles, left side, fig. S1, and Databases S7 and S13) that have been reported to interact with the targets of the 446 siRNA hits from Fig. 1A. Of the 292 protein targets of the hits from the small-molecule screen from Fig. 1A, 108 were associated with proteins that were targeted by hits from the siRNA screen (fig. S1, middle bioinformatic overlap, and Databases S10 and S13). Relative to a random sampling of proteins targeted by siRNAs that failed to meet the hit criteria (Databases S8, S9, and S11), the targets of the hits from our siRNA screen show a significantly higher percentage of interaction with proteins associated with hits from the small-molecule screen ($P \leq 0.001$, Chi-

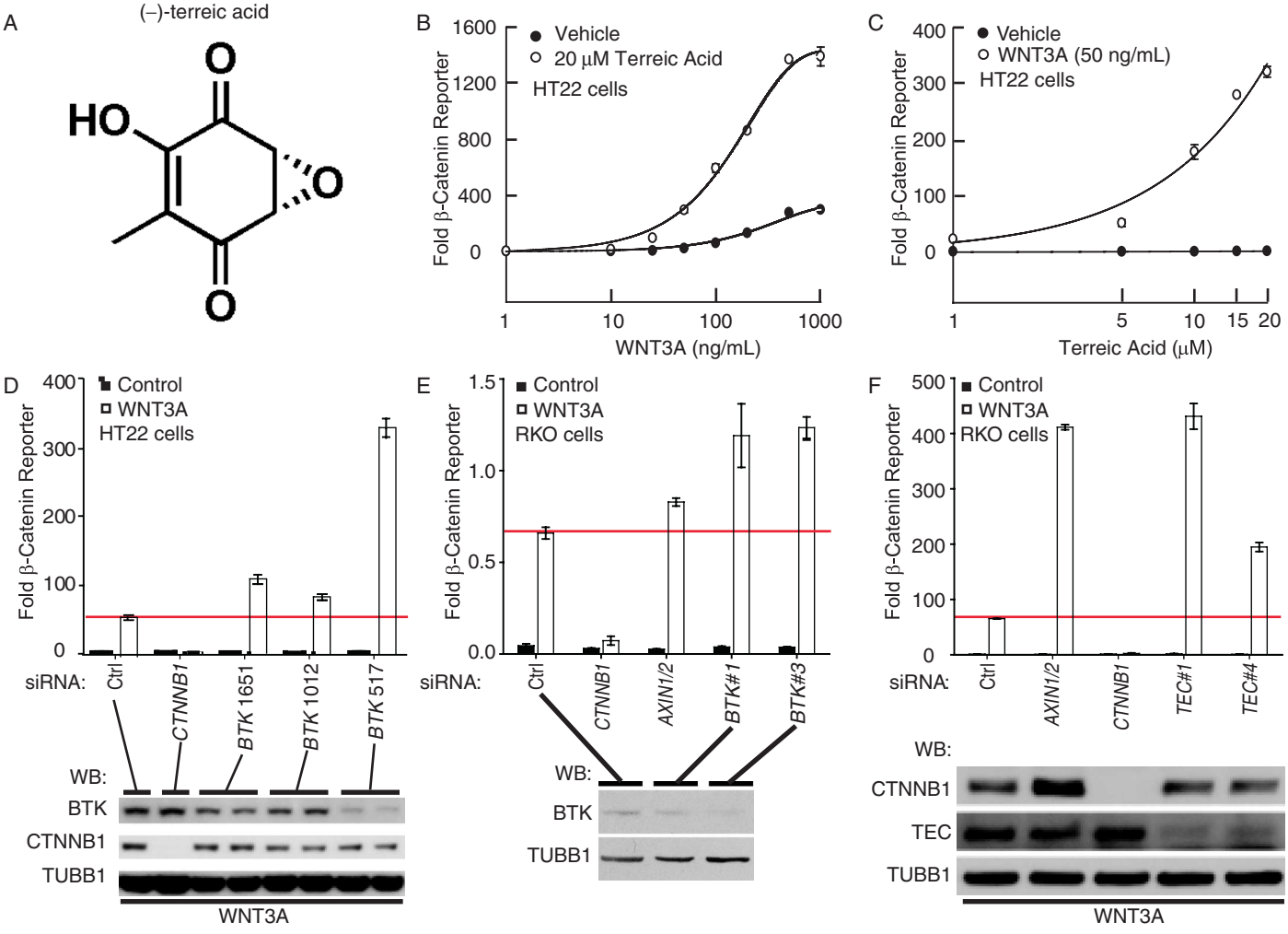

Fig. 2. Terreic acid and BTK validation in HT22 and RKO cells. (**A**) Structure of (–)-terreic acid. (**B**) HT22 cells stably expressing a β-catenin–activated reporter (BAR) upstream of firefly luciferase and a constitutive *Renilla* luciferase cassette were treated overnight with vehicle or 20 μM terreic acid and several concentrations of WNT3A. Ratios of firefly to *Renilla* luciferase were quantified, normalized to untreated control, and plotted. (**C**) HT22 cells carrying BAR were treated with vehicle or WNT3A (50 ng/ml) and several concentrations of terreic acid. Cell lysates were analyzed and plotted as in (B). Terreic acid increases the efficacy and potency of WNT3A in stimulating a transcriptional reporter of the Wnt–β-catenin pathway (B and C). (**D** to **F**) HT22 and RKO cells stably expressing BAR were transiently transfected with the indicated siRNA oligonucleotides. Forty-eight hours after transfection, the cells were treated with either WNT3A-conditioned media or control (Ctrl)-conditioned media. The following day, cell lysates were analyzed and plotted as in (B). Error bars represent standard deviation from the mean for three replicates. These data are representative of three independent experiments. *BTK* (top panels, D and E) and *TEC* (top panel, F) siRNAs synergize with WNT3A in activating Wnt–β-catenin signaling in HT22 and RKO cells. Western blot analysis with the indicated antibodies was performed on lysates of cells treated with the indicated siRNAs (bottom panels, D to F).

squared two-tailed test). Among the additional protein targets that we have identified as Wnt–β-catenin regulators by bioinformatic integration, many are functionally redundant with other proteins, thus validating the utility of the approach.

BTK is a negative regulator of Wnt–β-catenin signaling

BTK was identified in both screens as a negative regulator of the Wnt–β-catenin signaling. Data from the high-throughput, small-molecule screen revealed that (–)-terreic acid (terreic acid), a small-molecule inhibitor of BTK (*22*), enhances Wnt–β-catenin signaling (Fig. 1B, arrow, and Table 1). Data from the siRNA screen independently confirmed that BTK is a negative regulator of the Wnt–β-catenin pathway (Fig. 1B, arrow, and Table 1). Although BTK was targeted by hits in each of these screens, it had not been previously linked to Wnt–β-catenin signal transduction. In light of its unknown roles in this signaling pathway, and because BTK is linked to the B cell deficiency disorder, X-linked aggammaglobulinemia (*23*, *24*), we focused on validating and characterizing this unexpected role for BTK in regulating Wnt–β-catenin signaling.

Focusing first on the HT22 cells used for the small-molecule screen, we performed pharmacological studies of two independent chemical inhibitors of BTK and queried the effects of additional siRNAs directed against *Btk*. Dose-response curves of terreic acid and WNT3A in HT22 BAR cells revealed that terreic acid increased the efficacy and potency of WNT3A in activating BAR (Fig. 2, B and C). Three independent siRNAs targeting *Btk* variably reduced its expression as monitored by Western blot (bottom panel, Fig. 2D), and all three siRNAs synergized with WNT3A in activating BAR in HT22 cells (top panel, Fig. 2D). To validate BTK as a negative regulator of Wnt–β-catenin signaling in the RKO colonocytes used for the primary siRNA screen, we tested two independent siRNA sequences that target *BTK*. Both siRNAs decreased the abundance of the BTK protein in unstimulated cells (bottom panel, Fig. 2E) and synergized with WNT3A in activating BAR in RKO cells (top panel, Fig. 2E). We conclude that BTK negatively regulates Wnt–β-catenin signaling in both HT22 and RKO cells.

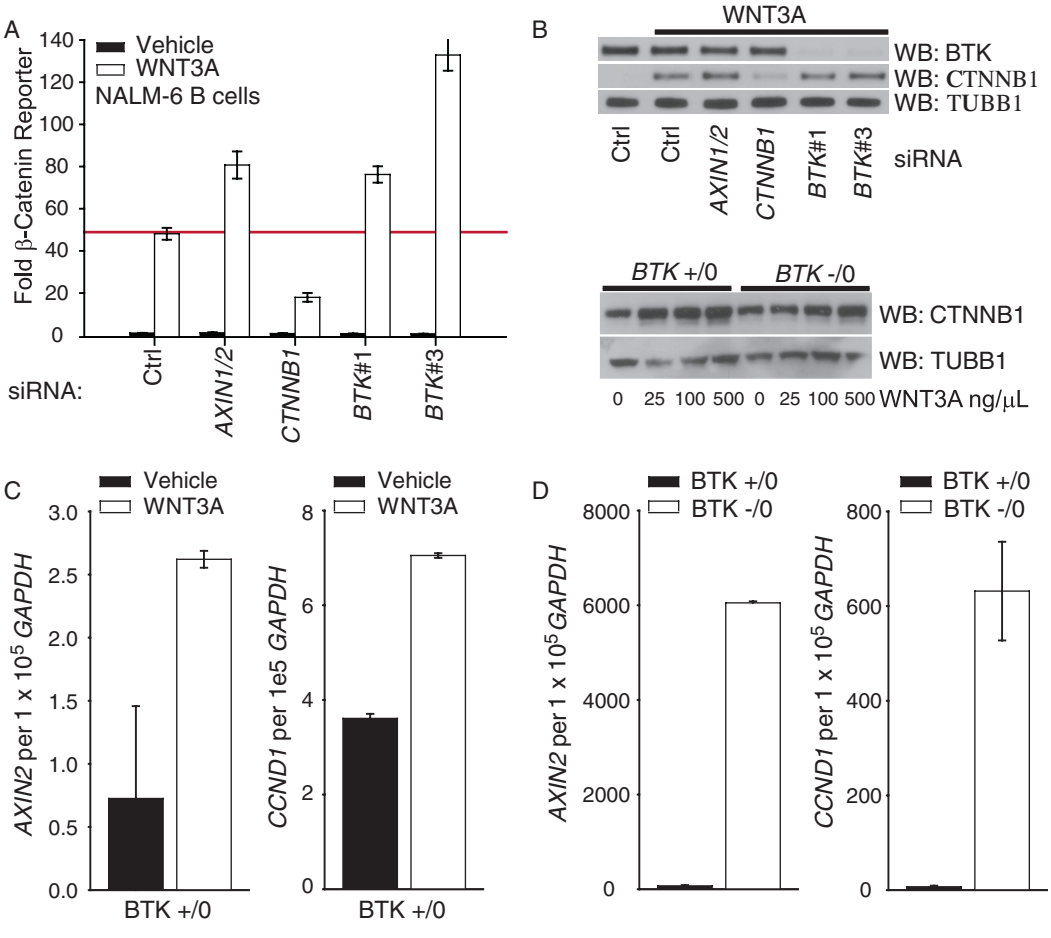

Fig. 3. The agammaglobulinemia-linked kinase, BTK, inhibits Wnt–β-catenin signaling. (**A**) NALM-6 B cells stably expressing BAR upstream of firefly luciferase and expressing a constitutive reporter that drives *Renilla* luciferase were transiently transfected with the indicated siRNA oligonucleotides. Forty-eight hours after transfection, the cells were treated with either WNT3A-conditioned medium or control medium. The following day, amounts of firefly luciferase were quantified, normalized to that of *Renilla* luciferase, and all data were plotted as fold change over untreated control siRNA. Error bars represent standard deviation from the mean for three replicates. These data are representative of three independent experiments. (**B**) Top: NALM-6 B cells were transfected with siRNAs targeting the indicated mRNAs. Two days after transfection, the cells were incubated overnight with WNT3A-conditioned media. Cell lysates were Western blotted with antibodies against BTK, CTNNB1, and TUBB1. Bottom: BTK does not decrease the abundance of CTNNB1 in unstimulated or WNT3A-stimulated cells. Patient-derived B cells were treated overnight with recombinant WNT3A at the indicated concentrations, lysed for protein analysis, and subjected to Western blotting for CTNNB1 and TUBB1. (**C**) Control B cells from normal patients were treated with recombinant WNT3A (100 ng/ml) overnight and processed for qPCR to show that Wnt–β-catenin signaling is intact in normal B cells. (**D**) Untreated B cell lines derived from patients lacking functional *BTK* and wild-type control B cells were processed for qPCR, showing that Wnt–β-catenin signaling is elevated in the absence of stimulation in BTK-deficient B cells. In both (C) and (D), the B cell cDNA was amplified with primers targeting *GAPDH* (*glyceraldehyde-3-phosphate dehydrogenase*) and the Wnt–β-catenin targets *AXIN2* and *CCND1*. The number of copies of *AXIN2* and *CCND1* were averaged, normalized to 1×10^5 copies of *GAPDH* amplified from the same sample, and plotted. These data represent three independent replicates in three independent experiments.

The bioinformatic overlap between small-molecule and siRNA screens (fig. S1) identified a second published target of terreic acid, the BTK paralog TEC, raising the question of whether TEC, like BTK, modulates Wnt–β-catenin signaling. Although TEC did not meet the hit criteria of the siRNA primary screen, careful examination of the data showed that two of three pooled siRNAs against TEC showed synergy with WNT3A (Databases S2 and S3). Because TEC is a BTK paralog and also a target of terreic acid, we validated two independent siRNA sequences that decreased the abundance of the TEC protein (bottom panel, Fig. 2F) and found that TEC inhibition activates expression of BAR (top panel, Fig. 2F). On the basis of independent assays that used either multiple siRNAs or a small-molecule inhibitor in two different cell lines, we conclude that TEC kinases can function to negatively regulate Wnt–β-catenin–mediated activation of the BAR reporter.

BTK inhibits Wnt–β-catenin signaling in B lymphocytes

To investigate whether *BTK* inhibits Wnt–β-catenin signaling in B cells, we stably integrated the BAR reporter into the human pre-B cell line, NALM-6 (NALM-6:BAR) (*25*). To validate that the Wnt–β-catenin pathway is intact in NALM-6 B cells, we stimulated NALM-6:BAR cells with WNT3A in the presence of a control siRNA or in the presence of siRNAs that target *CTNNB1* or the genes encoding the destruction complex components AXIN1 and AXIN2. As expected, treatment of NALM-6:BAR cells with WNT3A promoted BAR activity and this activity was inhibited by siRNAs directed against *CTNNB1* and was enhanced by siRNAs directed against *AXIN1* and *AXIN2* (Fig. 3A). As predicted by a model in which BTK negatively regulates Wnt–β-catenin signaling, two independent siRNAs that target *BTK* and substantially deplete the BTK protein (Fig. 3B, top panel) synergized with WNT3A in activating BAR in B cells (Fig. 3A).

If our hypothesis that BTK negatively regulates Wnt–β-catenin signaling is valid, then expression of endogenous β-catenin target genes should be elevated in cells genetically deficient for *BTK*, mirroring the results obtained with the synthetic target gene, BAR. To investigate whether perturbation of *BTK* affects expression of endogenous Wnt–β-catenin target genes, we analyzed immortalized cells derived from patients with X-linked agammaglobulinemia (*26*), which are deficient for functional BTK. Wild-type control B cells stimulated with WNT3A increased the abundance of CTNNB1 (Fig. 3B, bottom panel) and the abundance of the *AXIN2* and *CCND1* transcripts, two previously reported transcriptional targets of CTNNB1 (Fig. 3C). Consistent with BTK inhibiting Wnt–β-catenin signaling in B cells, the messenger RNAs (mRNAs) for *AXIN2* and *CCND1* were increased in the absence of exogenous Wnt stimulation in patient-derived *BTK* mutant B cells (open bars, Fig. 3D) compared to wild-type controls (filled bars, Fig. 3D). Thus, the Wnt–β-catenin signaling pathway is intact in B cells, and expression of known target genes of this pathway is inhibited by BTK.

To query whether BTK specifically regulates CTNNB1 downstream of its destruction complex, we monitored the steady-state and Wnt-stimulated abundance of CTNNB1 in two separate cell systems lacking BTK. The abundance of CTNNB1 was identical in WNT3A-stimulated NALM6 B cells treated with control siRNA or siRNA targeting *BTK* (Fig. 3B, top panel). Furthermore, the abundance of CTNNB1 in wild-type B cells and those lacking functional *BTK* was similar in response to increasing concentrations of WNT3A (Fig. 3B, bottom panel). Thus, in B cells, BTK inhibits expression of transcriptional targets of the Wnt–β-catenin signaling pathway without affecting the abundance of CTNNB1.

btk inhibition synergizes with Wnt–β-catenin signaling in zebrafish

Wnt–β-catenin signaling regulates the development of anterior structures in developing zebrafish (*27*) (Fig. 4A), rendering it a useful model to evaluate the in vivo role for previously unidentified regulators of Wnt–β-catenin signaling identified in cell-based screens. We first established that zebrafish *btk* is expressed broadly before gastrulation and found that it is enriched in hematopoietic precursor cells at later stages (fig. S2, A to C). Upon microinjection of low amounts (1.5 pg) of *wnt8* RNA into one cell–stage zebrafish, 31% of the embryos developed with mild anterior truncations as expected (Fig. 4B). Concomitant microinjection of *wnt8* RNA with either of two distinct splice-blocking morpholino oligonucleotides (4 ng) (see fig. S2E for validation) that target zebrafish *btk* resulted in a synergistic increase in the severity of anterior truncations (Fig. 4B and fig. S2D). As the phenotypic effects of low doses of *wnt8* RNA are enhanced by mor-

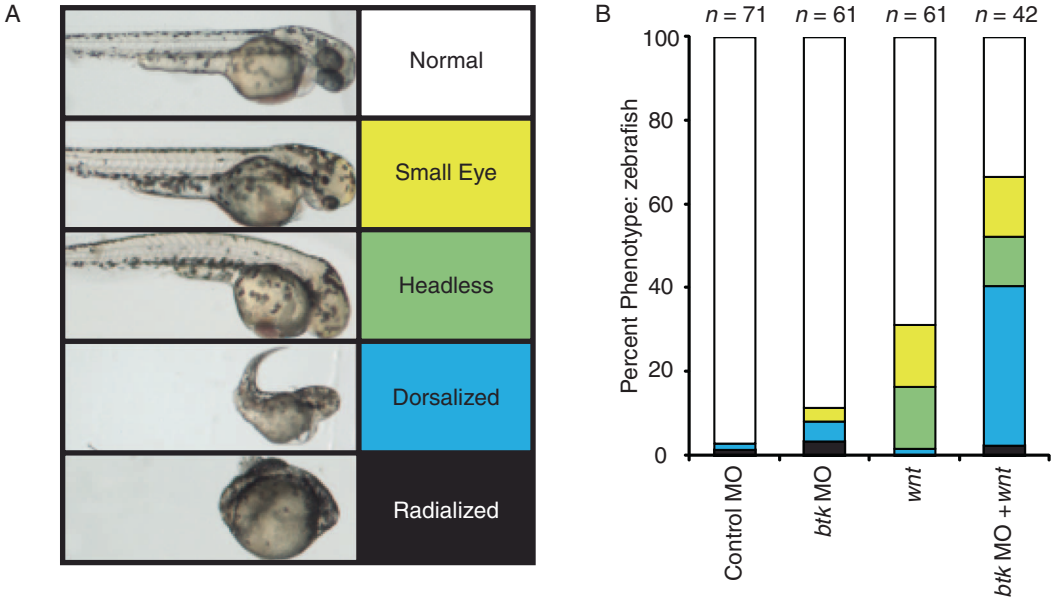

Fig. 4. *btk* silencing synergizes with Wnt–β-catenin signaling during the development of zebrafish embryos. (**A**) Injection of *wnt8* mRNA into one cell–stage zebrafish embryos causes anterior truncation in zebrafish by 24 hours after fertilization. The severity of the phenotype depends on the dose of *wnt8* mRNA; we characterize anterior truncation phenotypes as small eye, headless, dorsalized, or radialized. (**B**) Embryos injected with *btk* morpholino oligonucleotides (MO) displayed more anterior truncations than those injected with control MO. Additionally, embryos co-injected with *wnt8* mRNA (1.5 pg) and *btk* MO (4 ng) exhibited increases in the number and severity of anterior truncation phenotypes relative to co-injection with control MO. These data are representative of four independent experiments.

pholinos targeting *btk*, these in vivo results strongly suggest that blockage of *btk* splicing in the embryos leads to elevated Wnt–β-catenin signaling. Thus, in zebrafish, as in cultured cells, Btk negatively regulates Wnt–β-catenin signaling.

Proteomic analysis links BTK to the CTNNB1 partner CDC73

To further investigate the mechanisms by which BTK inhibits Wnt–β-catenin signaling, we screened for binding partners of BTK by affinity purification–mass spectrometry. We found that members of the PAF elongation complex (WDR61, PAF1, and CDC73) copurified with BTK (Fig. 5A, fig. S3A, and Database S16). Because CDC73 was previously reported to bind CTNNB1 and to be required for maximal transcription of Wnt–β-catenin target genes (*9*), the interaction between BTK and CDC73 was validated by several approaches. Epitope-tagged BTK and CDC73 proteins copurified from HEK293T cells (Fig. 5B). Similarly, immunoprecipitation of endogenous CDC73 from NALM-6 B cells showed coimmunoprecipitation of BTK relative to control (Fig. 5C). Demonstrating that these proteins interact directly, recombinant glutathione-*S*-transferase (GST)–BTK pulls down recombinant His-tagged CDC73 under stringent conditions in vitro (Fig. 5D). In conclusion, both endogenous and overexpressed BTK and CDC73 are detected in protein complexes in cells, and interact directly in vitro.

We then used tandem affinity purification of CDC73 and mass spectrometry to identify its binding partners in HEK293T cells (Database S17). Because BTK is not expressed in the HEK293T cells used for the CDC73 mass spectrometry experiments, BTK was not detected in the CDC73 affinity purification despite these proteins interacting directly in vitro and in vivo in NALM-6 B cells. Consistent with the hypothesis that CDC73 has a nuclear function, it copurified with several nuclear factors, including CTR9, LEO1, WDR61, and PAF1, all of which are components of the PAF transcription elongation complex (fig. S3B and Database S17). The protein-protein interaction data also reveal that both BTK and CDC73 interact with several other proteins that regulate transcriptional elongation, including the FACT complex members SUPT16H, SSRP1, and elonginA (TCEB3) (fig. S3B and Database S17). Additionally, both BTK and CDC73 bind the membrane-localized proteins SIT1, PIP5K1A, and GRB2 (fig. S3B). We conclude that BTK and CDC73 physically interact and share diverse binding partners.

CDC73 negatively regulates Wnt–β-catenin signaling in B cells

To investigate the functional role of CDC73 in Wnt–β-catenin signaling, we performed loss-of-function analysis with multiple siRNAs targeting *CDC73* in several cell types stably expressing the BAR reporter. In contrast to pre-

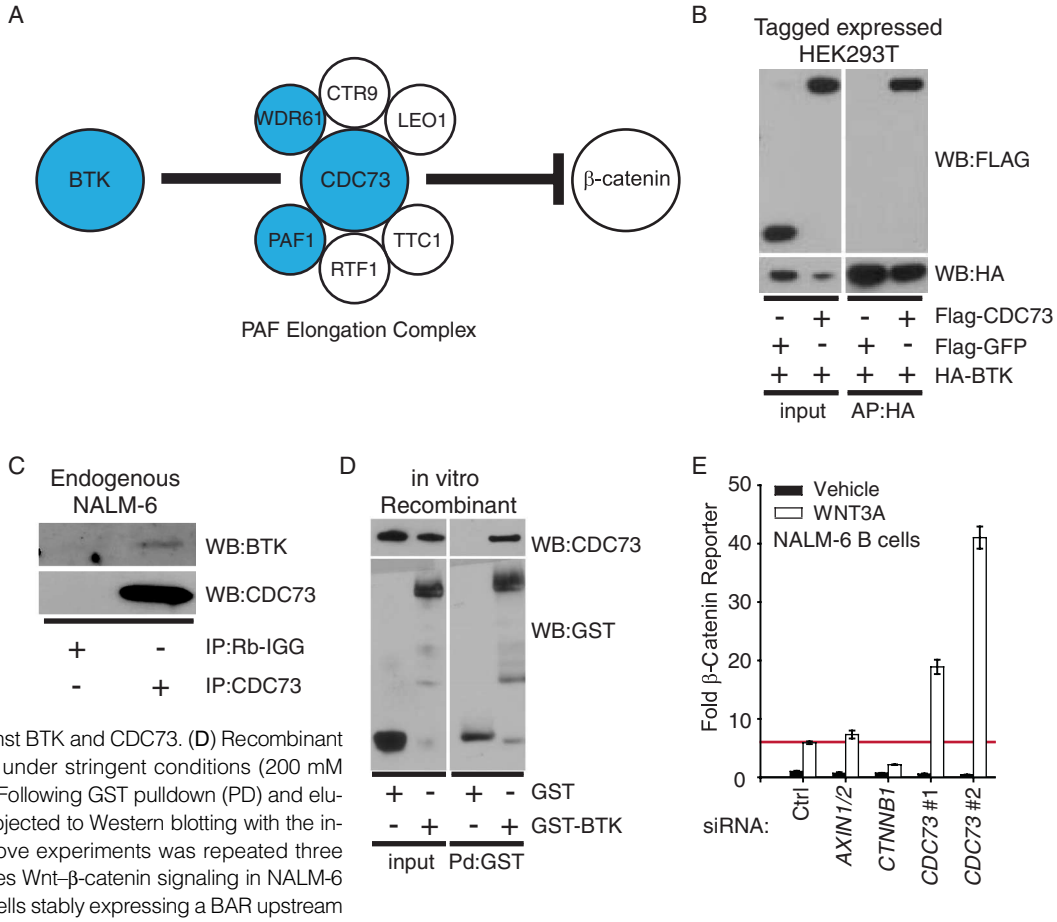

Fig. 5. Proteomics data and biochemical assays link BTK to CDC73. (**A**) Schematic illustrating the physical linkage between BTK, the PAF elongation complex, and β-catenin. BTK was affinity purified and subjected to liquid chromatography–tandem mass spectrometry to identify binding partners. The PAF complex members WDR61, CDC73, and PAF1 (blue) copurified with BTK, and the PAF complex is known to physically interact with CTNNB1 (*9*). (**B**) FLAG-tagged GFP and CDC73 were co-expressed with Glue-tagged BTK in HEK293T cells. Glue-BTK was affinity purified (AP) from cell lysates with streptavidin beads and then Western blots (WB) were probed for the indicated antibodies. (**C**) NALM-6 B cells were lysed and then immunoprecipitated (IP) with the indicated antibodies. The immunoprecipitates were analyzed by Western blot with antibodies against BTK and CDC73. (**D**) Recombinant His-tagged CDC73 was incubated under stringent conditions (200 mM NaCl) with GST or GST-BTK in vitro. Following GST pulldown (PD) and elution, the protein complexes were subjected to Western blotting with the indicated antibodies. Each of the above experiments was repeated three times. (**E**) CDC73 negatively regulates Wnt–β-catenin signaling in NALM-6 B cells. NALM-6 B cells. NALM-6 B cells stably expressing a BAR upstream of firefly luciferase and expressing a constitutive reporter that drives *Renilla* luciferase were transiently transfected with the indicated siRNA oligonucleotides. Forty-eight hours after transfection, the cells were treated with either WNT3A- or control-conditioned medium. The following day, firefly luciferase was quantified, normalized to that of *Renilla* luciferase, and all data were plotted as fold change over activity in untreated control siRNA-treated cells. Error bars represent standard deviation from the mean for three replicates. These data are representative of three independent experiments.

vious reports (*9*), siRNA-mediated attenuation of *CDC73* expression synergized with WNT3A to activate BAR in NALM-6 B cells (Fig. 5E) and RKO colonocytes (fig. S4A). To reconcile the conflicts between our RKO and NALM-6 data and published studies, we repeated the experiments with the HEK293T cells used in the previous study (*9*) and confirmed that CDC73 is required for maximal activation of BAR in those cells (fig. S4B). Together, our data indicate that depending on the context, CDC73 can either inhibit or enhance a Wnt–β-catenin signal. We further conclude that, like BTK, CDC73 negatively regulates the Wnt–β-catenin signal transduction cascade in B cells and RKO colorectal cancer cells.

BTK modulates the abundance of CDC73 in B cells

Because BTK and CDC73 physically interact and because both proteins negatively regulate Wnt–β-catenin signaling, we explored whether BTK is necessary for the inhibition of β-catenin signaling by CDC73. We compared the abundance of CDC73 in normal cells (immortalized B cell lines from normal patients and B cells from wild-type mice) with its abundance in cells deficient for functional *BTK* (immortalized B cell lines from X-linked agammaglobulinemia patients and $Btk^{-/0}$:$Tec^{-/-}$ mice). In both cell lines (Fig. 6A) and primary B lineage cells lacking functional *BTK* (Fig. 6B), the abundance of CDC73 was decreased relative to that in wild-type cells. The abundance of Cdc73 in *Btk*-deficient chicken DT40 B cells (*28*) transduced with viral vectors expressing green fluorescent protein (GFP) or BTK was also increased in cells expressing exogenous BTK, but not GFP (Fig. 6C).

To clarify how BTK modulates CDC73 abundance, we investigated the effect of *BTK* on *CDC73* RNA and protein stability. Quantitative polymerase chain reaction (qPCR) analysis of patient-derived B cells showed that *CDC73* transcripts were unexpectedly more abundant in cells lacking *BTK* (Fig. 6D), thus ruling out the possibility that *BTK* increases CDC73 abundance by increasing *CDC73* transcription. To address whether the presence of *BTK* affected the stability of the CDC73 protein, we performed pulse-chase analysis of CDC73 in patient-derived B cells. Autoradiographs of CDC73 immunoprecipitates from the patient-derived B cells showed a prominent band at 60 kD immediately after a pulse of ^{35}S-labeled amino acid (Fig. 6E, top panel). To determine whether the 60-kD band was indeed CDC73, we isolated it from a silver-stained gel of a parallel sample and conducted in-gel digestion and mass spectrometry, which verified that the band was CDC73 (Database S18). In support of the conclusion that the presence of BTK correlates with increased

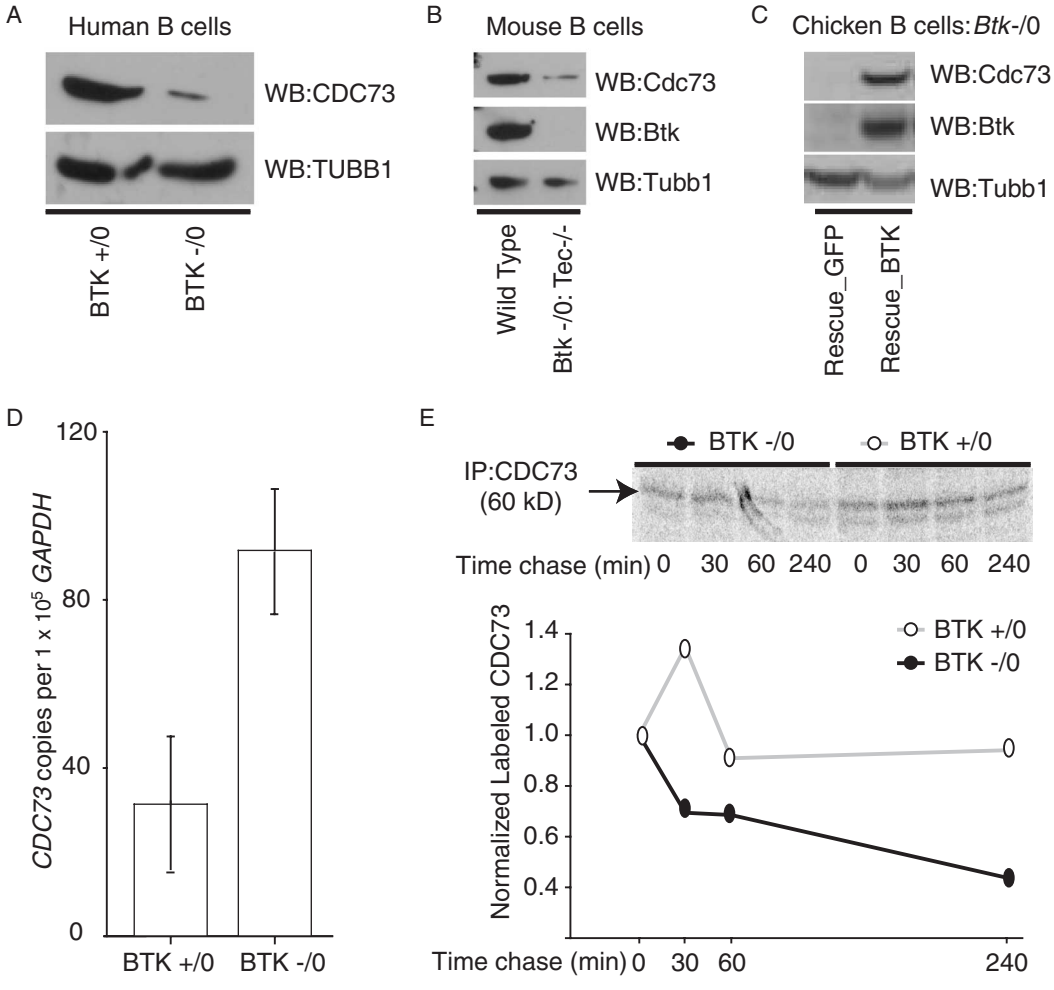

Fig. 6. BTK is associated with increased abundance of CDC73. (**A**) Patient-derived B cells and wild type control cells were lysed and analyzed by Western blot (WB) for CDC73 and TUBB1. (**B**) Blood cells were isolated from the bone marrow of wild-type and BTK$^{-/0}$:TEC$^{-/-}$ mice and B cells were cultured to homogeneity in the presence of IL-7. Lysates were subject to Western blotting with the indicated antibodies. (**C**) BTK-deficient chicken B cells transduced with BTK or GFP were lysed and analyzed by Western blot for CDC73, BTK, and TUBB1. (**D**) The presence of BTK correlates with decreased abundance of *CDC73* RNA in unstimulated patient-derived B cell lines. B cell lines derived from a patient lacking functional BTK and a wild-type sibling were processed for qPCR. The B cell cDNA was amplified with primers for *GAPDH* and *CDC73*. *CDC73* copy number was averaged, normalized to 1 × 10^5 copies of *GAPDH* amplified from the same sample, and plotted. These data represent three independent replicates of the same experiment. (**E**) The presence of *BTK* is associated with increased CDC73 stability. Pulse-chase analysis of CDC73 was performed and the indicated time points were processed for autoradiography. The gel was exposed (top) and the 60-kD band identified as CDC73 was quantified (bottom). The autoradiograph is representative of three independent experiments.

CDC73 stability, the CDC73 protein was reproducibly more stable in wild-type controls than in patient-derived cells that lack functional BTK (Fig. 6E; bottom panel). Thus, BTK appears to be required to maintain the abundance of CDC73, which in turn regulates Wnt–β-catenin signaling.

DISCUSSION

By coupling small-molecule screening and siRNA screening we have identified several regulators of the Wnt–β-catenin signaling pathway. Although this approach is inadequate for genome-wide identification of regulators of a signaling pathway, the integration of two independent screening technologies allowed us to avoid imposing somewhat arbitrary cutoffs as the threshold for candidate hits in either screen while reducing false positives caused by off-target effects specific to either type of screen.

The role of BTK in Wnt–β-catenin signaling

This study presents the initial evidence linking BTK with Wnt–β-catenin signaling. However, examination of the literature reveals data consistent with a role for BTK as a negative regulator of Wnt–β-catenin signaling in vivo. In addition to its well-documented role in X-linked agammaglobulinemia, abrogation of BTK function is also associated with acute lymphoblastic leukemia. Aberrant, dominant-negative *BTK* transcripts lacking the region encoding the functional kinase domain are found in a high percentage of patients with acute lymphoblastic leukemia (*29*). Coincidentally, the promoters of several protein inhibitors of Wnt–β-catenin signaling are hypermethylated in a large percentage of patients with acute lymphoblastic leukemia (*2*). These patients exhibit increased abundance of nuclear β-catenin, and elevated transcription of Wnt–β-catenin target genes compared to the expression in normal patients (*2*). The data from patients with acute lymphoblastic leukemia are one case where defective BTK and hyperactive Wnt–β-catenin signaling are observed in the same disease.

A second example where *BTK* loss of function can be correlated with a condition characterized by excessive Wnt–β-catenin signaling is colorectal carcinoma. Activating mutations of the Wnt–β-catenin signaling pathway are thought to be the major contributor to the development of colorectal cancer (*3*). In addition to the data that BTK is expressed in multiple colorectal carcinoma cell lines (Fig. 2) (*30*), a statistically high number of cases of colorectal carcinoma have been observed in patients with X-linked agammaglobulinemia (*31*, *32*). Although it is generally thought that the increases in colorectal cancer observed in X-linked agammaglobulinemia patients are due to aberrant immunological function in the colon, it is possible that hyperactive Wnt–β-catenin signaling could also play a role. Given our data that BTK and TEC can inhibit Wnt–β-catenin signaling and are present in several tissue types, further investigation of the links between BTK and Wnt–β-catenin signaling is warranted.

In addition to its well-published role in B cell receptor signaling (*26*), a distinct nuclear pool of BTK interacts with nuclear factors and influences transcriptional regulation (*33*). Our epistasis data show that BTK regulates Wnt–β-catenin signaling downstream of the destruction complex (Fig. 3B), and affinity purification–mass spectrometry shows that BTK binds to several elongation components, including multiple members of the FACT and PAF elongation complexes (fig. S3). The PAF complex, CDC73 in particular, is a good candidate to mediate BTK's inhibition of Wnt–β-catenin signaling because, like BTK, CDC73 regulates the transcriptional response to Wnt (Fig. 4F) and does not regulate the stability of CTNNB1 (*9*). Because multiple B cell lines lacking functional *BTK* show decreased abundance of CDC73, and CDC73 inhibits the Wnt–β-catenin pathway in B cells, it is plausible that the increased Wnt–β-catenin signaling observed in these cells is explained by loss of CDC73.

CDC73 is reported to be a tumor suppressor gene contributing to hyperparathyroidism (*34*) and renal cell carcinoma (*35*). Consistent with a role as a tumor suppressor, CDC73 inhibits proliferation in some cell lines (*36*). Interestingly, CDC73 promotes proliferation in other cell lines (*37*), suggesting a context-specific role in cell proliferation. Our data similarly indicate that the function of CDC73 depends on context. In colonocytes and B cells, CDC73 negatively regulates Wnt–β-catenin signaling; however, in HEK293T cells, CDC73 is required for maximal response to WNT3A stimulus (fig. S4B) (*9*). Further investigation of the mechanism by which CDC73 exerts cell type–specific phenotypes will be important for understanding how it acts as a tumor suppressor and how it regulates Wnt–β-catenin signaling.

Conclusion

By integrating a cell-based siRNA screen for modulators of a β-catenin–dependent reporter with an independent cell-based screen for small-molecule modulators of the reporter, we identified several previously unknown regulators of the Wnt–β-catenin signal transduction pathway, including the B cell kinase BTK. Our observations show that BTK negatively regulates the transcription of Wnt–β-catenin target genes by contributing to the stability of CDC73, a component of the PAF transcriptional elongation complex that inhibits Wnt–β-catenin target gene expression in B cells. Combined with previous reports (*3*, *31*, *32*, *34*, *35*), our data suggest a role for dysregulated Wnt–β-catenin signaling in diseases associated with abnormalities in *BTK* and *CDC73*.

MATERIALS AND METHODS

Reagents

Human *CDC73* and *BTK* complementary DNAs (cDNAs) were created with standard PCR-based cloning strategies. Detailed descriptions, maps, and sequences of the pGLUE and pCDNA-FLAG backbones and the pBARLS (*38*) vector can be found on the Moon Lab Web site (http://faculty.washington.edu/rtmoon/). The β-catenin–activated reporter (pBAR) is a lentiviral plasmid that contains 12 TCF binding sites (5′-AGATCAAAGG-3′) separated by distinct 5–base pair linkers (*16*) upstream of a minimal *thymidine kinase* promoter and the firefly luciferase open reading frame. The reporter also contains a separate phosphoglycerate kinase promoter that constitutively drives the expression of a puromycin resistance gene. To engineer stable cell lines that express pBAR or the BTK and CDC73 expression constructs, cells were either transfected (BTK and CDC73) or infected (pBAR-LS) with unconcentrated virus, and selected with puromycin (2 μg/ml). Transient transfection of siRNA was performed with RNAiMAX, as directed by the manufacturer (13778-075, Invitrogen). All siRNA sequences used are listed in table S1. LFM-A13 (435300, Calbiochem), terreic acid (581810, Calbiochem), and recombinant WNT3A (GF160, Millipore) were acquired from commercial sources.

B cell lines

NALM6 human pre-B cells (*25*, *39*) and transformed human peripheral blood B cells obtained from normal human donors (LDN) and from patients with X-linked agammaglobulinemia [LDX (*26*)] were grown in RPMI 1640 with 10% fetal bovine serum and 55 μM β-mercaptoethanol. BTK-deficient chicken B cells were a gift from T. Kurosaki and were grown as described (*28*). To stably transduce BTK-deficient DT40 cells, retrovirus was generated by cotransfection of MSCV retroviral plasmids (containing either murine Btk or the empty vector control and a cis-linked GFP marker) and a 10A1 pseudotype packaging plasmid into HEK293T cells with Fugene6 (Roche Applied Science, Indianapolis, IN). Viral supernatants were used to infect BTK-deficient DT40 cells. Stably transduced GFP^+ cells were isolated by cell sorting with a FACSAria with FACSDiva software (BD Biosciences). Primary murine B cells were expanded from bone marrow

cells extracted from age-matched $Tec^{-/-}Btk^{-/-}$ and C57BL6 wild-type mice. Bone marrow cells were plated at 1 million/ml in Dulbecco's modified Eagle's medium (DMEM) supplemented with 10% FBS, 55 μM β-mercaptoethanol, and mouse interleukin-7 (IL-7; 10 ng/ml) (PeproTech, Rocky Hill, NJ) and grown at 37°C in 5% CO_2. Every 2 days, cells were passaged to maintain 1 million cells/ml in fresh media and IL-7.

High-throughput, small-molecule screen

Screening was performed using the facilities of the Chemical Biology Platform at the Broad Institute in Cambridge, MA. Compounds dissolved in DMSO were obtained from the vendors listed in the complete data set in Database S1. For the primary screen, performed in duplicate, HT22 cells stably expressing BAR were cultured in growth medium (DMEM/10% FBS/1% antibiotic). Three thousand cells per well were transferred to 384-well clear-bottom plates (Corning) in 30 μl of growth medium. The following day, 100 nl of compound and 10 μl of either growth medium or WNT3A-conditioned medium (EC_{50} dose) was transferred to the cells. The next day, each well was imaged with transmitted light with the ImageXpress Micro (Molecular Devices) followed by the addition of 10 μl of Steady-Glo (Promega) and quantification of luminescence with an EnVision Multilabel plate reader (PerkinElmer). Viability was scored by analyzing the ImageXpress images. As described in detail by Seiler *et al.* (*40*), each compound well received an algebraically signed *Z* score corresponding to the number of standard deviations it fell above or below the mean of a well-defined mock-treatment distribution of DMSO controls. *Z* score–normalized data from the growth media stimulus group were sorted by average percent change. The fold increase over the background of DMSO controls for each treatment was also calculated. Each hit that had a *Z* score greater than 2 was selected for bioinformatic comparison with the siRNA screen.

High-throughput siRNA screen

The siRNA screen was performed as previously described (*41*), with minor modifications. Briefly, cells were reverse-transfected in 384-well plates, with a final concentration of pooled siRNA at 100 μM. Seventy-two hours after transfection, firefly luciferase and AlamarBlue staining were quantified. All siRNAs were designed according to standard rules of asymmetry. *Z* scores were calculated for all siRNAs relative to several control treatments. For each gene, the *Z* scores for all siRNAs (three to seven independent sequences per gene) were averaged. The genes that had mean *Z* scores greater than 2 were selected for bioinformatic overlap with the small-molecule screen.

Overlap of the siRNA screen and small-molecule screen

STITCH (*17*) was used to generate a list of possible protein targets of the hits (Database S4) found in the small-molecule screen. Experimental, database-derived, and text-mining predictions were used with a required confidence of 0.4 and a network depth of 1 to generate a list of binary interactions (Database S6). STRING (*21*) was used to generate a list of first-order interactors of the hits (Database S7) from the focused siRNA screen. Experimental and database-derived predictions were used with a required confidence of 0.7 and a network depth of 1 to generate a list of binary interactions (Database S7). The STITCH and STRING binaries were then overlaid to identify the set of genes in common with each network (Database S10). The set of binary interactions from the STITCH and STRING searches were combined (Database S12 Tab: CombinedBinary) and imported in Cytoscape version 2.6 (*42*) to generate a combined network (see Database S13 for the Cytoscape network). The individual STRING, STITCH, and Overlap networks were separated from the combined network by using an attribute file (Database S12 Tab: STR_STI_Overlap_Attribute). Small molecules were distinguished from genes with a node shape attribute (Database S12 Tab: CompoundAttribute). Small-molecule hits were characterized by the polarity of their activity in the screen with a node color attribute as Compound Up (Database S12 Tab: ScoreAttribute). Proteins in the networks were characterized based on their presence in the siRNA screen, whether they were scored as a hit or not, and the polarity of the activity of the hits in the screen with a node color attribute as siRNA NOT A HIT, siRNA Up, or siRNA Down (Database S12 Tab: ScoreAttribute).

Affinity purification, mass spectrometry, and data analysis

The lysis and wash conditions for all biochemical experiments were 1% NP-40, 20 mM Hepes, 150 mM NaCl, 2 mM dithiothreitol, protease inhibitors (11836170001, Roche), and phosphatase inhibitors (04906837001, Roche). For affinity purification–mass spectrometry experiments, minor modifications were made to a previously reported scheme (*15*). Affinity purification was performed by incubation of lysates generated from 2×10^8 cells with 50 μl of packed M2 FLAG resin (A2220, Sigma Aldrich). Protein complexes were washed several times in lysis buffer and twice in amonium bicarbonate buffer (50 mM). The protein complexes were eluted with FLAG peptide (100 μg/ml; F3290, Sigma Aldrich) and 0.1% RapiGest (186001860, Waters Corp.) in ammonium bicarbonate (50 mM). Following trypsinization and before mass spectrometry, RapiGest was cleaved in 250 mM HCl at 37°C for 30 min. Endogenous immunoprecipitation and tagged affinity purifications were performed by using standard conditions. The lysis and immunoprecipitation for the pulse-chase were performed in high-salt radioimmunoprecipitation buffer (250 mM NaCl, 20 mM Hepes, 1% NP-40, 0.25% sodium deoxycholate, and 0.1% SDS). The remainder of the pulse-chase was performed using standard protocols. For endogenous pull-down assays and Western blotting, we used the following antibodies: monoclonal antibody against FLAG M2 (F2555, Sigma Aldrich); polyclonal antibodies against hemagglutinin (1867423; Roche), GFP (ab290, Abcam), β-catenin (9562; Cell Signaling Technology), CDC73 (A300-170A, BETHYL Labs), LEO1 (A300-175A, BETHYL Labs), and BTK (C-20, Santa Cruz Biotechnology); and monoclonal antibody TUBB1 (T7816, Sigma Aldrich).

To generate the protein interaction networks for BTK and CDC73, raw mass spectrometry data were searched with SEQUEST (Thermofisher), and proteins were identified by use of the Institute for Systems Biology's transproteomic pipeline (*43*). Protein data were culled by removal of all proteins present in a list of commonly observed mass spectrometry contaminants (*13*). For each protein, two independent affinity purifications were performed in 293T cells. All prey proteins that were present in both preparations or were identified by three independent peptides in one preparation were kept for further analysis. To identify literature interactions for BTK and CDC73, all prey proteins from the culled lists were submitted to STRING. The STRING output, several manually curated literature interactions, and the primary mass spectrometry data were used to generate Cytoscape (*42*) interactomes (Cytoscape files S14 and S15).

In vitro binding experiments

Recombinant GST-BTK (1.5 pM; HZ-2014, Humanzyme) or recombinant GST was incubated for 15 min at 37°C with 1.5 pM of recombinant His-CDC73 in 250 mM NaCl. The recombinant protein mixtures were incubated with <10 μl of GST beads (17-0756-01, GE Healthcare), and washed four times (250 mM NaCl, 50 mM Hepes). The beads were incubated with elution buffer (250 mM NaCl, 50 mM Hepes, and 20 mM glutathione), and the proteins were collected by centrifugation through a spin column (89879, Pierce). Recombinant His-CDC73 and GST were generated using standard techniques.

RNA isolation, reverse transcription and quantitative real-time PCR

Total RNA from tissue culture cells or zebrafish embryos was harvested in Trizol (15596-018, Invitrogen) reagent. The RNA was further purified in RNEasy spin columns (74106, Invitrogen). Single-stranded cDNA was synthesized from 1 μg of total RNA with Superscript III (11752-050, Invitrogen) and random hexamers. Real-time PCR was performed with the Roche Light Cycler II instrument and software (Roche Diagnostics). PCR was performed in duplicate with the LightCycler FastStart DNA SyBr Green kit (12239264001, Roche). The PCR conditions are as follows: 35 cycles of amplification with 1 s denaturation at 95°C, and 5 s annealing at 58°C. A template-free negative control was included in each experiment.

Fish experiments

For zebrafish morpholino oligonucleotide experiments, 0.5 to 4 ng of morpholino oligonucleotide was co-injected with 1 pg of *wnt8* mRNA at the one cell–stage (GeneTools). The morpholino oligonucleotide sequences are *btk*-MO1 (5′-GACAATCTGTCAAAGAGATAAAACA), and *btk*-MO2 (5′-ACCCCTGGTGGAATGATAATACA TG). To assay for splice blocking, we used the following primers that flank the targeted splice site and controlled with primers directed against zebrafish *bactin* (*btk* MO1 F 5′-ACCTCCTGACCGGCACTAC, R 5′-CTGCATCAG GTCCTTGTTG A; *btk* MO2 F 5′-TCAGGAGGTCAAGCAGGCTA, R 5′-TCAGCT ATAACGGTCATGCCTA; and *bactin* F 5′-GGTATGGGACAGAAAGACAG, R 5′-AGAGTCCATCACGATACCAG). In situ hybridization for two distinct regions of the *btk* gene was performed using standard techniques with the following amplifying primers: probe 1 (F 5′-CGCACCAATGACTACCAATG, R 5′-TTCAGCAGACATC CATTTGC) and probe 2 (F 5′-ATGGCAGACA-GAGTTCTGGA, R 5′-TTATATCT CTTGCATACTGAAAAGCA).

SUPPLEMENTARY MATERIALS

www.sciencesignaling.org/cgi/content/full/2/72/ra25/DC1
Fig. S1. Bioinformatic overlap of independent small-molecule and siRNA screens reveals previously unidentified regulators of Wnt–β-catenin signaling.
Fig. S2. Zebrafish expression and loss-of-function data.
Fig. S3. Protein interaction networks for BTK and CDC73.
Fig. S4. Context-dependent regulation of Wnt–β-catenin signaling by CDC73.
Table S1. Sequences of siRNA sense strands.
Table S2. Descriptions of supplementary database files.
Databases S1 to S18.

REFERENCES AND NOTES

1. R. T. Moon, A. D. Kohn, G. V. De Ferrari, A. Kaykas, WNT and β-catenin signalling: Diseases and therapies. *Nat. Rev. Genet.* **5**, 691–701 (2004).
2. J. Román-Gómez, L. Cordeu, X. Agirre, A. Jiménez-Velasco, E. San José-Eneriz, L. Garate, M. J. Calasanz, A. Heiniger, A. Torres, F. Prosper, Epigenetic regulation of Wnt-signaling pathway in acute lymphoblastic leukemia. *Blood* **109**, 3462–3469 (2007).
3. T. Reya, H. Clevers, Wnt signalling in stem cells and cancer. *Nature* **434**, 843–850 (2005).
4. H. Clevers, Wnt/β-catenin signaling in development and disease. *Cell* **127**, 469–480 (2006).
5. C. E. Macsai, B. K. Foster, C. J. Xian, Roles of Wnt signalling in bone growth, remodelling, skeletal disorders and fracture repair. *J. Cell. Physiol.* **215**, 578–587 (2008).
6. N. C. Inestrosa, E. M. Toledo, The role of *Wnt* signaling in neuronal dysfunction in Alzheimer's Disease. *Mol. Neurodegener.* **3**, 9 (2008).
7. C. Y. Logan, R. Nusse, The Wnt signaling pathway in development and disease. *Annu. Rev. Cell Dev. Biol.* **20**, 781–810 (2004).
8. F. J. Staal, T. C. Luis, M. M. Tiemessen, WNT signalling in the immune system: WNT is spreading its wings. *Nat. Rev. Immunol.* **8**, 581–593 (2008).
9. C. Mosimann, G. Hausmann, K. Basler, Parafibromin/Hyrax activates Wnt/Wg target gene transcription by direct association with β-catenin/Armadillo. *Cell* **125**, 327–341 (2006).
10. N. Barker, H. Clevers, Mining the Wnt pathway for cancer therapeutics. *Nat. Rev. Drug Discov.* **5**, 997–1014 (2006).
11. Q. Zhang, M. B. Major, S. Takanashi, N. D. Camp, N. Nishiya, E. C. Peters, M. H. Ginsberg, X. Jian, P. A. Randazzo, P. G. Schultz, R. T. Moon, S. Ding, Small-molecule synergist of the Wnt/β-catenin signaling pathway. *Proc. Natl. Acad. Sci. U.S.A.* **104**, 7444–7448 (2007).
12. R. Firestein, A. J. Bass, S. Y. Kim, I. F. Dunn, S. J. Silver, I. Guney, E. Freed, A. H. Ligon, N. Vena, S. Ogino, M. G. Chheda, P. Tamayo, S. Finn, Y. Shrestha, J. S. Boehm, S. Jain, E. Bojarski, C. Mermel, J. Barretina, J. A. Chan, J. Baselga, J. Tabernero, D. E. Root, C. S. Fuchs, M. Loda, R. A. Shivdasani, M. Meyerson, W. C. Hahn, CDK8 is a colorectal cancer oncogene that regulates β-catenin activity. *Nature* **455**, 547–551 (2008).
13. M. B. Major, B. S. Roberts, J. D. Berndt, S. Marine, J. Anastas, N. Chung, M. Ferrer, X. Yi, C. L. Stoick-Cooper, P. D. von Haller, L. Kategaya, A. Chien, S. Angers, M. MacCoss, M. A. Cleary, W. T. Arthur, R. T. Moon, New regulators of Wnt/β-catenin signaling revealed by integrative molecular screening. *Sci. Signal.* **1**, ra12 (2008).
14. R. DasGupta, A. Kaykas, R. T. Moon, N. Perrimon, Functional genomic analysis of the Wnt-wingless signaling pathway. *Science* **308**, 826–833 (2005).
15. S. Angers, C. J. Thorpe, T. L. Biechele, S. J. Goldenberg, N. Zheng, M. J. MacCoss, R. T. Moon, The KLHL12-Cullin-3 ubiquitin ligase negatively regulates the Wnt–β-catenin pathway by targeting Dishevelled for degradation. *Nat. Cell Biol.* **8**, 348–357 (2006).
16. M. B. Major, N. D. Camp, J. D. Berndt, X. Yi, S. J. Goldenberg, C. Hubbert, T. L. Biechele, A. C. Gingras, N. Zheng, M. J. MacCoss, S. Angers, R. T. Moon, Wilms tumor suppressor WTX negatively regulates WNT/β-catenin signaling. *Science* **316**, 1043–1046 (2007).
17. M. Kuhn, C. von Mering, M. Campillos, L. J. Jensen, P. Bork, STITCH: Interaction networks of chemicals and proteins. *Nucleic Acids Res.* **36**, D684–D688 (2008).
18. C. Yost, M. Torres, J. R. Miller, E. Huang, D. Kimelman, R. T. Moon, The axis-inducing activity, stability, and subcellular distribution of β-catenin is regulated in *Xenopus* embryos by glycogen synthase kinase 3. *Genes Dev.* **10**, 1443–1454 (1996).
19. A. N. Billin, H. Thirlwell, D. E. Ayer, β-catenin-histone deacetylase interactions regulate the transition of LEF1 from a transcriptional repressor to an activator. *Mol. Cell. Biol.* **20**, 6882–6890 (2000).
20. S. Hino, C. Tanji, K. I. Nakayama, A. Kikuchi, Phosphorylation of β-catenin by cyclic AMP-dependent protein kinase stabilizes β-catenin through inhibition of its ubiquitination. *Mol. Cell. Biol.* **25**, 9063–9072 (2005).
21. L. J. Jensen, M. Kuhn, M. Stark, S. Chaffron, C. Creevey, J. Muller, T. Doerks, P. Julien, A. Roth, M. Simonovic, P. Bork, C. von Mering, STRING 8—A global view on proteins and their functional interactions in 630 organisms. *Nucleic Acids Res.* **37**, D412–D416 (2009).
22. Y. Kawakami, S. E. Hartman, E. Kinoshita, H. Suzuki, J. Kitaura, L. Yao, N. Inagaki, A. Franco, D. Hata, M. Maeda-Yamamoto, H. Fukamachi, H. Nagai, T. Kawakami, Terreic acid, a quinone epoxide inhibitor of Bruton's tyrosine kinase. *Proc. Natl. Acad. Sci. U.S.A.* **96**, 2227–2232 (1999).
23. S. Tsukada, D. C. Saffran, D. J. Rawlings, O. Parolini, R. C. Allen, I. Klisak, R. S. Sparkes, H. Kubagawa, T. Mohandas, S. Quan, J. W. Belmont, M. D. Cooper, M. E. Conley, O. N. Witte, Deficient expression of a B cell cytoplasmic tyrosine kinase in human X-linked agammaglobulinemia. *Cell* **72**, 279–290 (1993).
24. D. Vetrie, I. Vořechovský, P. Sideras, J. Holland, A. Davies, F. Flinter, L. Hammarström, C. Kinnon, R. Levinsky, M. Bobrow, C. I. Edvard Smith, D. R. Bentley, The gene involved in X-linked agammaglobulinaemia is a member of the *src* family of protein-tyrosine kinases. *Nature* **361**, 226–233 (1993).
25. R. Hurwitz, J. Hozier, T. LeBien, J. Minowada, K. Gajl-Peczalska, I. Kubonishi, J. Kersey, Characterization of a leukemic cell line of the pre-B phenotype. *Int. J. Cancer* **23**, 174–180 (1979).
26. A. C. Fluckiger, Z. Li, R. M. Kato, M. I. Wahl, H. D. Ochs, R. Longnecker, J. P. Kinet, O. N. Witte, A. M. Scharenberg, D. J. Rawlings, Btk/Tec kinases regulate sustained increases in intracellular Ca^{2+} following B-cell receptor activation. *EMBO J.* **17**, 1973–1985 (1998).
27. A. C. Lekven, C. J. Thorpe, J. S. Waxman, R. T. Moon, Zebrafish wnt8 encodes two wnt8 proteins on a bicistronic transcript and is required for mesoderm and neurectoderm patterning. *Dev. Cell* **1**, 103–114 (2001).
28. M. Takata, T. Kurosaki, A role for Bruton's tyrosine kinase in B cell antigen receptor-mediated activation of phospholipase C-γ2. *J. Exp. Med.* **184**, 31–40 (1996).
29. N. Feldhahn, P. Río, B. N. Soh, S. Liedtke, M. Sprangers, F. Klein, P. Wernet, H. Jumaa, W. K. Hofmann, H. Hanenberg, J. D. Rowley, M. Müschen, Deficiency of Bruton's tyrosine kinase in B cell precursor leukemia cells. *Proc. Natl. Acad. Sci. U.S.A.* **102**, 13266–13271 (2005).
30. J. Du, P. Bernasconi, K. R. Clauser, D. R. Mani, S. P. Finn, R. Beroukhim, M. Burns, B. Julian, X. P. Peng, H. Hieronymus, R. L. Maglathlin, T. A. Lewis, L. M. Liau, P. Nghiemphu, I. K. Mellinghoff, D. N. Louis, M. Loda, S. A. Carr, A. L. Kung, T. R. Golub, Bead-based profiling of tyrosine kinase phosphorylation identifies SRC as a potential target for glioblastoma therapy. *Nat. Biotechnol.* **27**, 77–83 (2009).
31. L. A. Brosens, K. M. Tytgat, F. H. Morsink, R. J. Sinke, I. J. Ten Berge, F. M. Giardiello, G. J. Offerhaus, J. J. Keller, Multiple colorectal neoplasms in X-linked agammaglobulinemia. *Clin. Gastroenterol. Hepatol.* **6**, 115–119 (2008).
32. J. W. van der Meer, R. S. Weening, P. T. Schellekens, I. P. van Munster, F. M. Nagengast, Colorectal cancer in patients with X-linked agammaglobulinaemia. *Lancet* **341**, 1439–1440 (1993).
33. J. Rajaiya, M. Hatfield, J. C. Nixon, D. J. Rawlings, C. F. Webb, Bruton's tyrosine kinase regulates immunoglobulin promoter activation in association with the transcription factor Bright. *Mol. Cell. Biol.* **25**, 2073–2084 (2005).

34. J. D. Carpten, C. M. Robbins, A. Villablanca, L. Forsberg, S. Presciuttini, J. Bailey-Wilson, W. F. Simonds, E. M. Gillanders, A. M. Kennedy, J. D. Chen, S. K. Agarwal, R. Sood, M. P. Jones, T. Y. Moses, C. Haven, D. Petillo, P. D. Leotlela, B. Harding, D. Cameron, A. A. Pannett, A. Höög, H. Heath III, L. A. James-Newton, B. Robinson, R. J. Zarbo, B. M. Cavaco, W. Wassif, N. D. Perrier, I. B. Rosen, U. Kristoffersson, P. D. Turnpenny, L. O. Farnebo, G. M. Besser, C. E. Jackson, H. Morreau, J. M. Trent, R. V. Thakker, S. J. Marx, B. T. Teh, C. Larsson, M. R. Hobbs, *HRPT2*, encoding parafibromin, is mutated in hyperparathyroidism–jaw tumor syndrome. *Nat. Genet.* **32**, 676–680 (2002).
35. J. Zhao, A. Yart, S. Frigerio, A. Perren, P. Schraml, C. Weisstanner, T. Stallmach, W. Krek, H. Moch, Sporadic human renal tumors display frequent allelic imbalances and novel mutations of the *HRPT2* gene. *Oncogene* **26**, 3440–3449 (2007).
36. G. E. Woodard, L. Lin, J. H. Zhang, S. K. Agarwal, S. J. Marx, W. F. Simonds, Parafibromin, product of the hyperparathyroidism-jaw tumor syndrome gene *HRPT2*, regulates cyclin D1/PRAD1 expression. *Oncogene* **24**, 1272–1276 (2005).
37. T. Iwata, N. Mizusawa, Y. Taketani, M. Itakura, K. Yoshimoto, Parafibromin tumor suppressor enhances cell growth in the cells expressing SV40 large T antigen. *Oncogene* **26**, 6176–6183 (2007).
38. T. L. Biechele, R. T. Moon, Assaying β-catenin/TCF transcription with β-catenin/TCF transcription-based reporter constructs. *Methods Mol. Biol.* **468**, 99–110 (2008).
39. H. W. Findley Jr., M. D. Cooper, T. H. Kim, C. Alvarado, A. H. Ragab, Two new acute lymphoblastic leukemia cell lines with early B-cell phenotypes. *Blood* **60**, 1305–1309 (1982).
40. K. P. Seiler, G. A. George, M. P. Happ, N. E. Bodycombe, H. A. Carrinski, S. Norton, S. Brudz, J. P. Sullivan, J. Muhlich, M. Serrano, P. Ferraiolo, N. J. Tolliday, S. L. Schreiber, P. A. Clemons, *ChemBank*: A small-molecule screening and cheminformatics resource database. *Nucleic Acids Res.* **36**, D351–D359 (2008).
41. S. R. Bartz, Z. Zhang, J. Burchard, M. Imakura, M. Martin, A. Palmieri, R. Needham, J. Guo, M. Gordon, N. Chung, P. Warrener, A. L. Jackson, M. Carleton, M. Oatley, L. Locco, F. Santini, T. Smith, P. Kunapuli, M. Ferrer, B. Strulovici, S. H. Friend, P. S. Linsley, Small interfering RNA screens reveal enhanced cisplatin cytotoxicity in tumor cells having both BRCA network and TP53 disruptions. *Mol. Cell. Biol.* **26**, 9377–9386 (2006).
42. P. Shannon, A. Markiel, O. Ozier, N. S. Baliga, J. T. Wang, D. Ramage, N. Amin, B. Schwikowski, T. Ideker, Cytoscape: A software environment for integrated models of biomolecular interaction networks. *Genome Res.* **13**, 2498–2504 (2003).
43. A. I. Nesvizhskii, A. Keller, E. Kolker, R. Aebersold, A statistical model for identifying proteins by tandem mass spectrometry. *Anal. Chem.* **75**, 4646–4658 (2003).
44. Nomenclature follows the HUPO standards for protein (Roman text in all capital letters) and gene and transcript names (italic text in all capital letters) for humans. Mouse, and chicken proteins and genes or transcripts are listed with initial capital letters in Roman and italic text, respectively. Zebrafish genes or transcripts are listed as lower case italic text.
45. This project has been funded in whole or in part with federal funds from the National Cancer Institute's Initiative for Chemical Genetics, NIH, under Contract No. N01-CO-12400 and has been performed with the assistance of the Chemical Biology Platform of the Broad Institute of Harvard and MIT. The content of this publication does not necessarily reflect the views or policies of the Department of Health and Human Service, nor does mention of trade names, commercial products or organizations imply endorsement by the U.S. Government. D.J.R. and K.S. were supported by a grant from the NIH (R01-HD037091). Additionally, R.T.M., R.G.J., T.L.B., W.H.C., N.D.C., and M.B.M. were supported by the Howard Hughes Medical Institute and by a grant from the Department of Defense (W81XWH-07-1-0367). We thank J. Berndt and A. Chien for critical reading of the manuscript; R. Kulikauskas for help with experiments not included in the final version; B. Sather for isolating primary B-cells for us from mice; and S. Norton and members of the Chemical Biology Platform for technical assistance.

Submitted 2 January 2009
Accepted 7 May 2009
Final Publication 26 May 2009
10.1126/scisignal.2000230
Citation: R. G. James, T. L. Biechele, W. H. Conrad, N. D. Camp, D. M. Fass, M. B. Major, K. Sommer, X. Yi, B. S. Roberts, M. A. Cleary, W. T. Arthur, M. MacCoss, D. J. Rawlings, S. J. Haggarty, R. T. Moon, Bruton's tyrosine kinase revealed as a negative regulator of Wnt–β-catenin signaling. *Sci. Signal.* **2**, ra25 (2009).